

14

Structural colours from self-assembled silica nanoparticles for textile coloration

Weihong Gao^{*1}, Huw Owens^{*2}, Muriel Rigout³

¹School of Fashion Technology, Shanghai University of Engineering Science, Shanghai, 201620, China.

²School of Materials, The University of Manchester, Manchester, M13 9PL, UK.

³School of Design, University of Leeds, Leeds, LS2 9JT, UK.

*Corresponding author

Outline

Introduction.....	308
<i>Structural colours from the self-assembled nanoparticle system.....</i>	308
Current applications of structural coloursfor textile industry.....	309
<i>Structurally coloured fibre/fabrics from bare nanoparticles.....</i>	309
<i>Structurally coloured fibres/fabrics by the coating of nanoparticles</i>	309
Structural coloration of textile materials from self-assembled silica nanoparticles	310
<i>Basic principles of structural colours in opals.....</i>	310
<i>Synthesis of silica nanoparticles by a solvent varying method.....</i>	311
<i>Artificial opal films by the self-assembly of silica nanoparticles.....</i>	312
<i>Structural coloration of textile fabrics by sedimentation of silica nanoparticles.....</i>	316
Conclusion and outlook.....	320
Acknowledgement.....	321
References.....	321

Introduction

Colour caused by the physical structure of a material, rather than the chemical molecules of conventional dyes and/or pigments, is generally referred to as 'structural colour'. In nature, structural colour is found in the animal [1] and mineral worlds [2]. The natural precious opal gemstone is probably the oldest and best-known example, with its brilliant play-of-colour when the stone is rotated [3]. It is known that the structural colour of the precious opal is due to the periodic nanostructure of highly-ordered tiny silica nanoparticles (SNPs)[4], which diffract the light that enters the opal material. This is a different process to how most surface colours are produced where light is more usually absorbed by dye and/or pigment molecules. Desirable aesthetic qualities could be achieved if the structural colours produced by natural precious opals could be replicated in the form of a film or a coating on textile substrates. Compared to the surface colour produced from traditional dyes and pigments, structural colour has several advantages including high intensity, high resistance to fading, a play-of-colour effect, easy tunability of colours, and less toxicity, as the raw materials for producing structural colours are normally benign colloidal nanoparticles such as silica or polymers spheres.

Structural colours from the self-assembled nanoparticle system

Generally speaking, natural opals can be classified into two types: precious and common (or potch) opals [2]. The precious opal may show brilliant iridescent structural colours from violet to red, as shown in Fig. 14.1(a). Such beautiful structural colours have also been achieved by self-assembling highly ordered SNPs into different coloured opal films, Fig. 14.1(b). Common opals are usually described as being 'opalescent' in colour due to the scattering of light, this is because the SNPs are not very uniform in size or not regularly arranged as seen in Fig. 14.1(c). The structural colour of precious opals may be described using a modified Bragg's diffraction equation, which is reliant on the SNPs forming a periodic structure where the ordered regions have a close-packed face-centred cubic (fcc) morphology. Fig. 14.1(d) shows the top view of an artificial opal film, where the hexagonal close-packed arrangement of SNPs represents the (1 1 1) plane of the fcc structure [5]. The square arrangement of SNPs on the cross-sectional view represents the (1 0 0) plane of the fcc structure, which can be seen in Fig. 14.1(e). Due to the uniform and ordered arrangement of the SNPs, a particular structural colour can be observed from the surface of the artificial opal film.

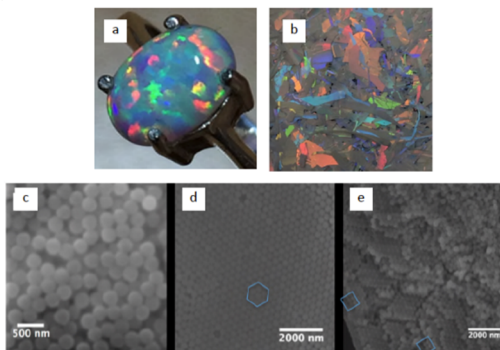


FIGURE 14.1

A natural precious opal ring bought from London Portobello antique market (a); a mixture of different coloured flakes of synthetic/artificial opal films (b); the SEM images of disordered (c); the ordered silica nanoparticles from the top (d); and the cross-sectional view of an artificial opal (e)

The study of replicating precious opals that have the ability to show various colours has become an active and wide-ranging research field. Scientists have successfully fabricated artificial opal Photonic Crystals (PCs) using bottom-up self-assembly techniques, such as natural sedimentation [6], vertical deposition [5], physical confinement [7], spin coating [8], and ink-jet printing [9]. The quality of the structural colour produced mainly depends on the uniformity of the nanoparticles and the regularity of the crystal structure [10]. In most studies, the adopted substrate for the self-assembly of the SNPs is smooth and flat, such as a glass surface or a silicon wafer, as this helps to produce a long-range ordered PC with high-quality structural colour. However, the application of structural colour to textile materials are just emerging [11].

Current applications of structural colours for textile industry

Although the basic fabrication technology of PCs is relatively mature, the applications of such materials in the textile industry are relatively rare which is probably because of the complex surface properties of textile materials. As one of the most important and interesting properties of artificial opals, structural colour allows the production of colours without traditional colorants (dyes/pigments) [12] – a very promising way to colour textile materials. Current research in this emerging area has focused on polymer-based nanoparticles, as they are organic and thus compatible with textile materials. Specifically, structurally coloured textile fibres have been fabricated by the self-assembly of uniform nanoparticles into a cylindrical shape with or without a core fibre. Structurally coloured fabrics are generally either produced from the knitting/weaving of structurally coloured fibres or by self-assembling nanoparticles on the surface of a piece of traditional textile fabric.

Structurally coloured fibres/fabrics from bare nanoparticles

Polymeric opal fibres have been produced by the extrusion of a prepared PS (polystyrene)-ALMA (allyl methacrylate)- PEA (polyethylacrylate) core-interlayer-shell polymer nanoparticle solution [13]. Elastomeric polymer opal fibre has many interesting features like stretch- and bend-tunability with associated features of reversible colour after deformation (stretching, bending or twisting). These fibres have also been knitted into fabrics. Most recently, Yuan *et al.* [14] have reported a fabrication method for structurally coloured colloidal fibres by the electro-spinning of P(St-MMA-AA) colloidal core-shell nanoparticles mixed with a polyvinyl acetate (PVA) solution; PVA was used as binding material to adhere the spheres. Green, yellow, and red-coloured colloidal crystal fibres have been fabricated by varying the nanoparticle diameter in the range of 220-280 nm. Moreover, Shang *et al.* [15] have produced one-dimensional chain-like photonic crystal fibre structures by embedding Fe₃O₄@C (iron-oxide core coated with carbon shell) super-paramagnetic colloidal nanocrystal clusters (SCNCs) into a polyacrylamide (PAM) matrix using an external magnetic field. The distance between each sphere in chain-like fibre structures can be reversibly changed through the elastic deformation of the matrix, resulting in a colour change of the fibre. It should be noted that it is difficult to form a fibre from only pure nanoparticles without the introduction of binding materials.

Structurally coloured fibres/fabrics by the coating of nanoparticles

By providing a base fibre/fabric, bare spheres such as silica or PS can be easily deposited and self-assembled onto the fibre/fabric surface, resulting in structurally coloured fibres/fabrics. Diao *et al.*

[16][17] produced red and golden structural colours from the surface of silk fabrics by the sedimentation of 270 nm- and 240 nm-sized PS spheres onto the fabric. Using a similar method, Zhou *et al.* have achieved a broader range of structural colours by the sedimentation of silica [18] and P(St-MAA) spheres [19] onto polyester fabrics. Instead of using relatively large fabric substrates, artificial opals can be also formed on the surface of tiny fibres to achieve structurally coloured fibres. Liu *et al.* [20] have reported an isothermal heating and evaporation-induced self-assembly method for fabricating structurally coloured glass fibres. In their work, uniform silica nanoparticles (215 nm, and 240 nm) were self-assembled onto the glass fibre's surface, resulting in green and blue coloured glass fibres. Zhou *et al.* [21] have created red, green, and blue structural colours by the self-assembly of PS spheres onto carbon fibres. Recently, Sun *et al.* [22] have produced structurally coloured PDMS fibres using PS spheres, they also designed chromatic patterns and fabrics using the coloured PDMS fibres. The colour of such PDMS fibres is tunable by varying the particle size as well as the strain of the fibre. It should be noted that, the structural colour produced by the sedimentation self-assembly methods is normally iridescent (angle-dependent); this limits the application of using nanoparticles for structural coloration in making dyes/pigments for the textile industry.

Structural coloration of textile materials from self-assembled silica nanoparticles

Basic principles of structural colours in opals

It is well known that for a crystal to diffract an X-ray beam, in order to get a constructive wave, the following Bragg equation must apply:

$$n = 2d\sin\vartheta_B \quad (1)$$

where d is the distance of the adjacent planes of atoms, λ is the X-ray wavelength, n is the order of the diffracted beams, and ϑ_B is the Bragg angle between the beams and the planes. With the aid of Bragg's law, the crystal structure can be analysed by viewing the resulting diffraction pattern, which consists of several diffracted spots with a certain arrangement and varied brightness. The Opal is a good example of light diffraction in nature and is analogous to how a crystal diffracts X-rays. Figure 14.2 shows a schematic of the Bragg diffraction of white light due to the structure of an opal crystal.

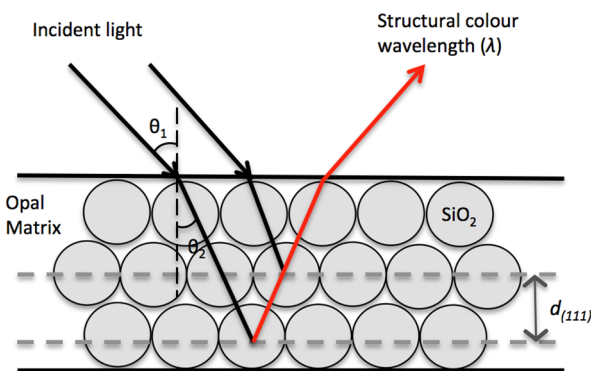


FIGURE 14.2

The Bragg diffraction of white light from an opal structure consisting of ordered SNPs

However, in the case of the opal, two modifications have to be made in order to apply Bragg's equation Eq. (1), which was derived from X-ray diffraction. Firstly, Bragg's equation has to be combined with Snell's law because of the different refractive indices (RI) between air and silica. Secondly, as the light travels in silica in a similar way to an X-ray travelling in a vacuum, this means the relative wavelength of light in an opal should be modified. Thus, the observed colour can be described in terms of its wavelength (λ) by a modified Bragg's equation [23]:

$$n\lambda = 2d_{(111)}(n_{eff}^2 \sin^2\vartheta_1)^{1/2} \quad (2)$$

or

$$n\lambda = 1.633d(n_{eff}^2 \sin^2\vartheta_1)^{1/2} \quad (3)$$

where λ is the wavelength of the reflectance peak of the coloured opal material, $d_{(111)}$ is the interplanar spacing between the (1 1 1) planes, d is the sphere diameter, n_{eff} is the effective refractive index (RI) of the opal material, and ϑ_1 is the angle between the normal and the incident light (the viewing angle). The longest achievable wavelength λ_{max} will occur at normal incidence, when $\sin \vartheta_1 = 0$ and $n = 1$; thus, Eq. (3) can be rewritten as [24]:

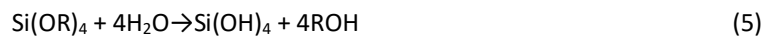
$$\lambda_{max} = 1.633dn_{eff} \quad (4)$$

For the given materials, the effective RI is a constant number, therefore, according to Eq. (4), it is clear that the wavelength of peak reflectance of the coloured opal has a positive correlation with the particle diameter d . The wavelength range of visible light is from approximately 400 nm to 700 nm. Therefore, there exist max-min limits for the particle diameter to give rise to a visible structural colour. It is found in our previous work [24] that the SNPs having the average diameter in the range of approximately 200 – 350 nm produced structural colours over the full visible spectrum. Particles outside this range produced an opalescent milky-white colour just as seen in potch opals. Specifically, SNPs that are smaller than 200 nm in diameter could reflect wavelengths in the ultraviolet (UV) region, while infra-red (IR) will be generated if the particles are larger than 350 nm.

Synthesis of silica nanoparticles by solvent varying method

The standard Stöber method

A commonly used method for preparing SNPs is based on the sol-gel Stöber method [25] which is a complex mechanism of nucleation and growth. The overall reaction can be written as follows in chemical Eqs. (5) and (6) in terms of the hydrolysis and condensation of silicon alkoxide, respectively:



where R represents the alkyl groups, i.e. $-\text{C}_n\text{H}_{2n+1}$. Research using the Stöber method generally uses tetraethyl ortosilicate (TEOS) as the precursor alkoxide, distilled water (DW) as the hydrolysing agent, ammonia (NH_3) acts as the catalyst, and absolute ethanol ($\text{C}_2\text{H}_5\text{OH}$) as the solvent.

Silica is one of the most frequently used spheres for making artificial opals due to its relative inert properties giving increased thermal and chemical stability compared to organic colloids, such as PS, PMMA, etc. However, the application of silica for the coloration of textile substrates has been rarely reported. Although the Stöber method of synthesizing uniform SNPs in the micron size range has been extensively studied [25][26][27] and large quantities of uniform SNPs samples can be bought

from commercial sources [28], the SNPs in a particular size range for structural colours are more challenging to achieve. This is probably due to the difficulties in controlling the complex two-stage reaction during the Stöber process that consists of the hydrolysis of TEOS and the condensation of silicic acid.

The solvent varying method

In our work, a straightforward one-step Stöber-based solvent varying (SV) method [29] was proposed to control the diameter of the silica particles for the purposes of the fabrication of structural colours on artificial opal films. The novel aspect of this method is to control the silica size and size distribution by only varying the volume of the initial solvent ethanol used, while fixing all the other reaction conditions such as the volume amounts of TEOS/NH₃(25%)/H₂O (6/8/3 ml), temperature (60°), reaction time (2 h), etc. Highly uniform SNPs with an average diameter of approximately 70 – 400 nm were produced using the SV method by varying the initial ethanol volume from 41 – 125 ml. An exponential equation, Eq. (7), was produced that fitted the relationship between the final measured particle diameter and the initial ethanol volume used, so that any target diameters in this size window can be predicted, which is given as:

$$d = 885.45\exp(-0.02[V_{EtOH}]) \quad (7)$$

where d is the diameter of the SNPs in nanometers (nm) and V_{EtOH} is the initial volume of ethanol added into the solution, which is given in millilitres (ml).

The SNPs prepared using the SV method were characterised using the dynamic light scattering (DLS) and scanning electron microscopy (SEM) techniques. The SEM shows that the prepared particles are uniform and spherical in shape, the diameter measured using the SEM micrographs were highly correlated to those obtained directly from the DLS instrument. The DLS also shows the narrow size distribution of the SNPs in solution as well as the small polydispersity index (PDI) (within 0.1), which indicates the high uniformity of the prepared SNPs. The SV method provides a facile method of controlling the size and uniformity of the silica spheres, thus allowing high-quality artificial opals films to be fabricated and structural colours to be tuned for further applications.

Artificial opal films by the self-assembly of silica nanoparticles

Particle size and uniformity are the main factors that affect the quality of the structural colours. However, the uniform SNPs have to be assembled in a well-ordered fashion, so that Bragg diffraction can occur. If there is no ordered structure, a white colour will be perceived from the SNPs bulk due to the scattering of white light regardless of the uniformity of the SNPs. Under certain forces, particles can continuously join together and form ordered 3D lattice structures, this is known as the self-assembly phenomenon. The process of sedimentation forms natural opals. Natural sedimentation by gravitation is the most straightforward self-assembly method and has been the most widespread method adopted in the literature to fabricate opals. In this work, structural colour has been achieved from the gravity sedimentation and thus self-assembly of SNPs on flat glass substrates prior to uneven fabric substrates. The purpose of producing opal films on glass substrates was to determine the SNP size range and optimum self-assembly conditions for the production of high-quality photonic crystals and hence structural colours.

Determination of size range for structural colours

From the modified Bragg's equation, Eq. (4), the wavelength and the particle size have a positive relationship, this limits the size range of particles that produce colours. In the natural precious opal the silica spheres normally have diameters ranging from 150 nm to 300 nm [3], in addition, it has been stated that the violet will appear at a particle size of 138 nm and red at 241 nm [30]. However, in this study, it has been found that the size range for producing a full range of colours was from 207 nm to 350 nm, Fig. 14.3. The red colour appears at 288 nm as shown in Fig. 14.3(d) and violet at about 210 nm as seen in Fig. 14.3(h). This is probably due to the larger amount of immobilized water in the artificial opal films, contributing to a smaller effective RI (n_{eff}) of the artificial opal matrix than the natural opals. It can be seen from Fig. 14.3 that with the increase of ethanol volume, the overall effect of the hue is changed gradually from red to violet. Although two pairs of samples, Figs. 14.3(a) and (b), (c) and (d), do not fit the trend of the colour change, but the particle size of the SNPs correlates with their colour appearance, namely bigger particles still produce colour with a longer wavelength, this is in agreement with Bragg's law. Since the prepared opal films only consist of simply stacking SNPs, and they are thus very fragile, small pieces of opal flakes can be produced easily. The blending of these pieces of flakes having different sized particles resulted in beautiful colour appearance as shown previously in Fig. 14.1(b).

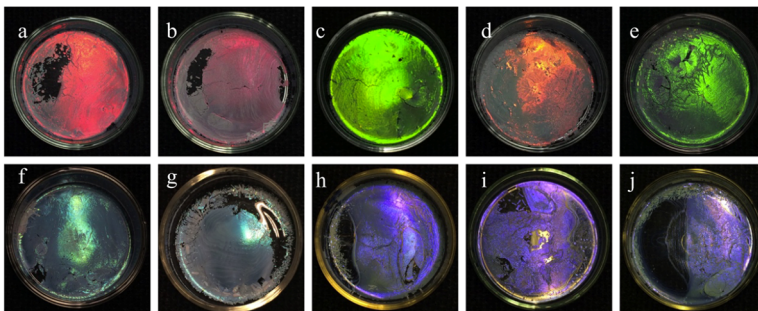


FIGURE 14.3

Structurally coloured opal films prepared using the SV method with an increased ethanol volume from 47 ml (a), 50 ml (b), 53 ml (c), 57 ml (d), 60 ml (e), 62 ml (f), 64 ml (g), 69 ml (h), 71 ml (i), and 73 ml (j). The size of the SNPs is 350 nm, 369 nm, 282 nm, 288 nm, 270 nm, 259 nm, 242 nm, 221 nm, 211 nm, and 207 nm for (a) – (j), respectively

Factors that affect the formation of opal films

During the sedimentation of the SNPs in the ethanol solvent, temperature is very important to the self-assembly of the photonic crystal, as it will affect the diffusion of the particles in the suspension. There exists an optimum temperature level to control the particle sedimentation and crystallization behaviour. Figure 14.4 shows structurally coloured films on glass petri dishes prepared using 267 nm-sized SNPs at different sedimentation temperatures from room temperature (RT) to 100 °C.

It can be observed from Fig. 14.4(a) that a ring was formed on the edge of the petri dish when the films were prepared at RT. This kind of ring formation is a common phenomenon observed on a flat surface of a solid substrate, which is caused by a particle accumulation on the edge of the droplet solution due to the high evaporation rate at the edge of the dish [31]. By increasing the temperature to 40 or 60 degrees, the ring shape was overcome, Figs. 14.4(b) and 4(c); with a further increase of

the temperature to 80 or 100 degrees, increasing defects are formed on the film in terms of numbers of holes, cracks, and unevenness, as shown in Figs. 14.4(d) and 4(e). This effect could be explained using Stoke's Law [6][32]:

$$V_s = d^2(\rho_s - \rho_f)g/18\eta \quad (8)$$

where V_s is the silica sedimentation velocity, d is the particle diameter, ρ_s and ρ_f are the silica particle and fluid densities, g is the gravitational acceleration which equals 9.81 m/s^2 , η is the fluid viscosity (ethanol in this case). It is known that ethanol has a lower viscosity η at higher temperatures [33], thus the silica sedimentation velocity V_s will increase when the temperature increases. To achieve better quality opals, V_s should be a constant and as low as possible, a higher temperature will increase the sedimentation rate which contributes to more defects. However, if this velocity were too low or close to zero, the self-assembly sedimentation may never occur.

From Fig. 14.4, it can be concluded that the optimum temperature was 40-60 °C, as it produced very uniform coloured films with fewer defects and without ring-shaped artefacts. This optimum range is in agreement with the work of several researchers, for example, Fu *et al.* [34] showed that assembled arrays formed at 50 °C have fewer defects than those at RT, and Im *et al.* [35] found that a higher temperature improves the quality of the colloidal crystal but a temperature greater than 60 °C resulted in a higher number of defects due to the high rate of crystal growth at high temperature levels.

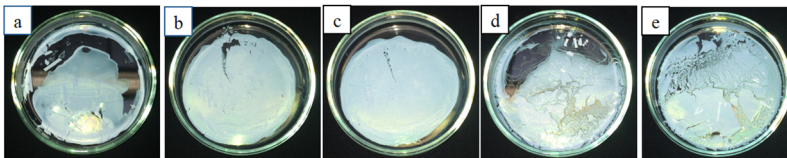


FIGURE 14.4

Structurally coloured opal films prepared in petri dishes at different drying temperatures of RT, 40, 60, 80, and 100 °C for (a) – (e), respectively

Tunable structural colour effect of opal films

The ultimate structural colour of an opal film cannot be directly observed from the white silica suspension; there is a process of colour change during the drying phase of the colloidal suspension [31][36]. Although the sedimentation of colloids in suspension under a gravitational field seems to be the simplest natural way to form 3D ordered arrays of spheres, it involves several processes such as gravitational settling, translational diffusion (or Brownian motion), and crystallization (nucleation and growth) [36]. In general, the self-assembly process has two main steps: the aggregation of spheres in suspension and then the crystallisation of the spheres. The colloidal spheres in the suspension will undergo a disorder-to-order phase transition to form a 3D ordered lattice. Lastly, the complete removal of the solvent by drying brings all the spheres together to form a close-packed fcc structured photonic crystal. It can be concluded from the self-assembly process that the final photonic crystal structure is not directly produced from the colloidal suspension, there are a few intermediate steps for the individual uniform spheres to join together and then form the final fcc structure which interferes with white light and produces structural colours.

Figure 14.5 shows the results of a self-assembly process of SNPs in suspension on a glass slide. In Fig. 14.5(a), 1 ml of suspension containing 207 nm SNPs was spread over the surface of a glass slide. The white milky opalescent colour of the initial suspension is due to the random Mie scattering of light

from the uniform SNPs. During the evaporation of the solvent, the colour at the edge of the suspension film changes from white to red, yellow, green, and blue, as seen in Figs. 14.5(b) – (g). This is because the distance between the spheres becomes smaller and smaller and so the observed wavelength (colour) shifts to a shorter wavelength, as predicted by the modified Bragg's law in Eq. (2). This phenomenon is known as the blue shift, as the wavelength of blue radiation is shorter than red. Figure 14.5(h) shows the ultimate uniform deep blue (violet) structural colour of the opal film when the solvent has been removed entirely.

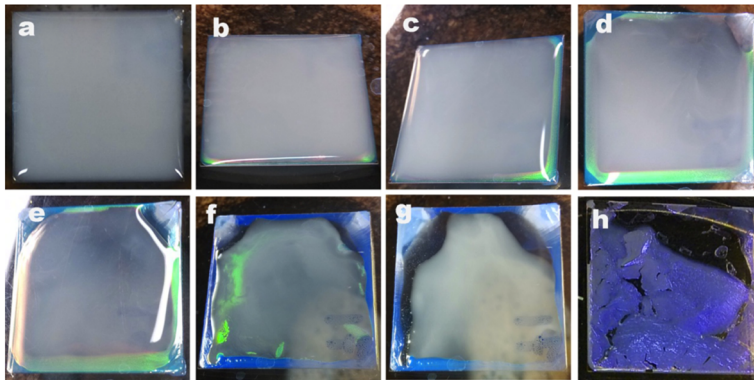


FIGURE 14.5

The self-assembly process of SNPs in suspension onto a glass slide to form coloured opal films, where (a) is the initial suspension, (b) - (g) represent the colour change of suspension film during drying, (h) shows the final colour

The natural opal produces a play-of-colour (POC) effect when rotated; its colour could change between red and blue when viewed at different angles. In our previous study [24], the effect of viewing angle to the structural colours of the artificial opal film was investigated.

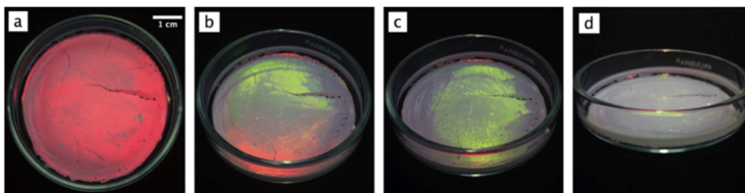


FIGURE 14.6

Images of a red coloured CC film self-assembled from SNPs of 350 nm diameter at viewing angles of 0° (a), 30° (b), 45° (c), and 90° (d); scale bars are the same as the one displayed in (a)

In Fig. 14.6, an opal film self-assembled from 350 nm sized SNPs shows the different structural colours of red, red—orange—green, green—white, and white at viewing angles of 0°, 45°, 60°, and 90°, respectively. At a 0° viewing angle, the normal incident angle, the silica opal film exhibits the intense and uniform structural colour of red, as seen in Fig. 14.6(a). When the viewing angle increased to 45°, different structural colours were clearly observed as shown in Fig. 14.6(b), where the opal film shows polychromatic structural colours including red, orange, and green. With a further increase of the viewing angle to 60°, the structural colour of the opal film reverts to a uniform hue but with a different colour of green, as seen in Fig. 14.6(c). The phenomenon of POC with viewing angle in an artificial opal is the same as in natural opals, and again it can be explained using the

modified Bragg's equation, Eq. (3). As the viewing angle θ increases and other parameters in the equation such as the particles' diameter d and refractive index n_{eff} , are fixed, the wavelength of the reflectance peak λ will decrease, contributing to an effective reduction in wavelength (blue-shift) of the structural colour. This explains how the colour of the opal film is gradually changed from red to green with the increase of viewing angle, as seen in Figs. 14.6(a)-6(c). In fact, total internal reflection will occur at a certain viewing angle (approaching 90°), this prevents the light source escaping from the material's surface [23], resulting in the extinction of the structural colour. This is confirmed in Fig. 14.6(d) where at a viewing angle of 90° , the opal film exhibits a white surface colour just as seen in normal silica powder.

Structural coloration of textile fabrics by sedimentation of silica nanoparticles

Due to the uniformity of the SNPs prepared using the SV method and the controlled self-assembly sedimentation, uniform and intense structural colours from opal films have been obtained on glass substrates. Using the same technique, structural colours have also been successfully achieved on textile fabrics. It has been demonstrated that a temperature of between 40 to 60 °C is favorable for a more uniform structural colour, so a higher temperature of 60 °C was used to accelerate the self-assembly process. However, due to the unevenness of the fabrics, short range ordered SNPs crystals would form on the fabric surface resulting in non-uniform and duller colours being perceived on the fabrics. The self-assembly behaviour and optical properties of SNP-coated fabrics have been studied in our previous work [37].

Self-assembly behaviour of SNPs on fabrics

The structure and self-assembly behavior of the SNPs on the substrates were studied by analysing SEM micrographs. Figure 14.7 shows one piece of woven fabric coated with 207nm-sized SNPs.

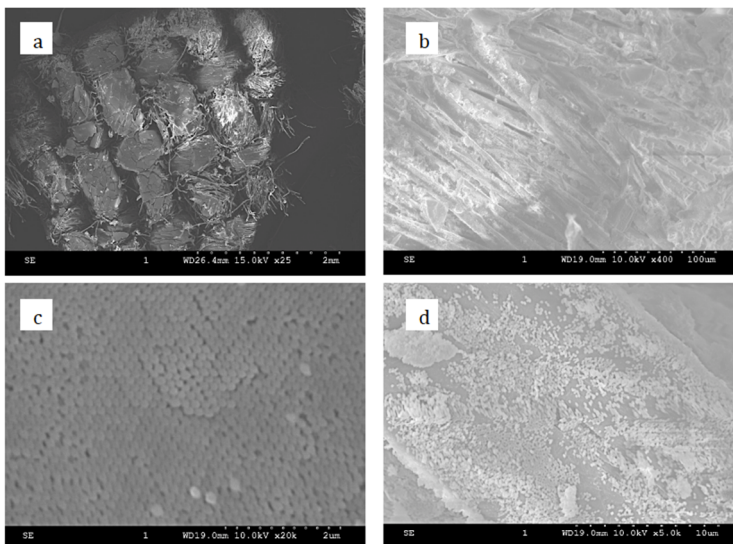


FIGURE 14.7

SEM images of 207 nm SNPs self-assembled on a woven fabric at magnification of 25 (a), 400 (b), 20 K (c), and 5 K (d), respectively

At the lower magnification of 25, Fig. 14.7(a), the uneven surface of the woven fabric structure can be clearly seen. It is noticeable that the photonic crystal structure did not cover the entire surface of the fabric as both silica blocks and individual floating yarns/fibres can be observed. Figure 14.7(b) shows a higher magnification of the silica blocks and gaps at a magnification of 400, where it can be seen that some local silica blocks are formed and there are some smaller isolated silica blocks floating on the yarns. The top view of the close-packed structure of the silica block is shown in Fig. 14.7(c), the hexagonal arrangement of SNPs corresponds to the (1 1 1) plane of an fcc crystals structure, which is the typical structure of the opal film formed on glass substrates. These thick and well-ordered silica blocks contribute to the structural colours due to Bragg diffraction in these regions. Figure 14.7(d) shows a magnified micrograph of SNP-coated fibres, SNPs are attached to the surface of a fibre, but the particles are not close-packed and there is only one layer of particles. There will be no Bragg diffraction from such an area, thus structural colours will not be generated. A white colour from the silica particles or the black background colour of the fibre can be possibly perceived instead.

Optical properties of the SNP-coated fabrics

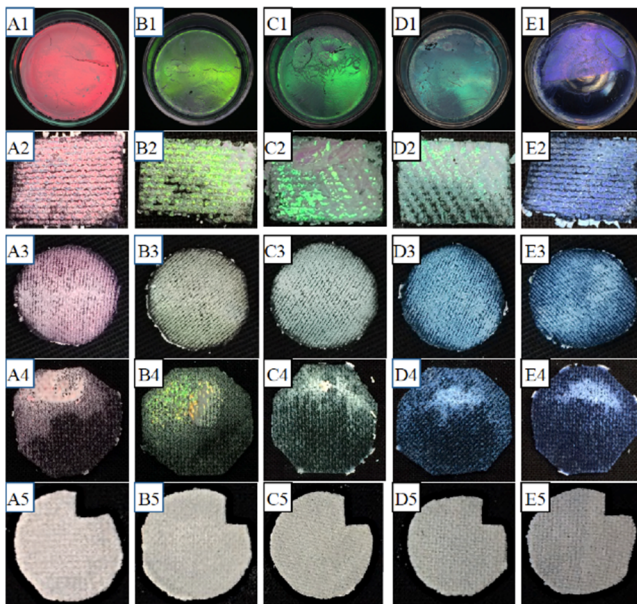


FIGURE 14.8

Structural colours from the self-assembled SNPs on different substrates: glass petri dish (A1-E1), small square (A2-E2) and bigger circular (A3-E3) black woven cotton, black (A4-E4) and white (A5-E5) knitted nylon. Samples in the vertical direction are treated with SNPs batch that prepared using the same recipe according to the SV method. Fabric samples in A2-E2 are treated using the same batches that had produced coloured film samples in A1-E1; the rest fabric samples are treated with newly prepared batches using the relevant recipes

In our previous work [24], structurally coloured silica opal colloidal crystal films have been fabricated and it was found that the structural colour was tuned by both the average diameter of the SNPs and the viewing angle. However, little has been reported about the structural colour properties of the silica photonic crystal on textile fabrics, specifically for cotton and nylon fabrics. In this work, a variety of structural colours were obtained by the self-assembly of SNPs on cotton and nylon fabrics and

their optical properties were determined. Figure 14.8 summarises all the structurally coloured samples prepared in our work [11][37][38].

It can be seen from Fig. 14.8 that the coloured opal films and coloured fabrics that were treated from the batch prepared using the same recipe present similar hue properties of red, yellow, green, cyan, and blue, the ethanol volumes used were 47 ml, 53 ml, 60 ml, 63 ml, and 67 ml, respectively. The SNP diameters measured using DLS were 350 nm (A1 and A2), 282 nm (B1 and B2), 270 nm (C1 and C2), 249 nm (D1 and D2), and 207 nm (D1 and D2); for the newly prepared batches, the measured SNP diameter was 342 nm (A3, A4 and A5), 287 nm (B3, B4 and B5), 262 nm (C3, C4 and C5), 233 nm (D3, D4 and D5), and 204 nm (E3, E4 and E5). In the SV method, due to the negative correlation between the ethanol and particle size, Eq. (7), the more volume of ethanol used the smaller the final particle that was formed. The colour in terms of its peak wavelength decreases according to a modified Bragg's Eq. (4), this is the reason for the blue shift of the coloured samples in Fig. 14.8.

The peak wavelength of coloured fabric samples in Figs. 14.8(A2)-8(E3) versus the applied SNP diameter are plotted in Fig. 14.9. A linear function fit was added with a zero intercept. If the particle diameter were zero, there is no peak wavelength due to Bragg diffraction, so the trend line should cross the origin. The linear function fit has the following expression, Eq. (8):

$$y = 1.8874x \quad (8)$$

where x represents the SNP diameter d , y is the related peak wavelength (λ_{max}). Considering the modified Bragg's law from Eq. (4), the slope of the function 1.8874 equals to $1.633n_{eff}$. Therefore, the effective RI n_{eff} of the SNP coated fabric was calculated as 1.16. The R-squared value of 0.902 validates the fitting of the linear function, which tends to confirm the occurrence of Bragg's diffraction of the ordered structures on the fabric.

The opal film samples in Figs. 14.8(A1)-8(E1) look more vivid, bright, and uniform, while the fabric samples are whiter, duller, and less uniform. The reason for the difference of structural colour between films and fabric could arise from the surface properties of the two different materials. Textile fabrics are normally complex in structure, uneven on the surface, and flexible in respect of dimensions. These factors make the self-assembly of SNPs more difficult to control. Therefore, SNPs can either self-assemble on the surface of the fabric surface to form thick photonic crystal blocks as seen in Fig. 14.6, or pass through the gaps between the yarns/fibres contributing to defects of the as-formed photonic crystals, and eventually leading to uneven structural colours.

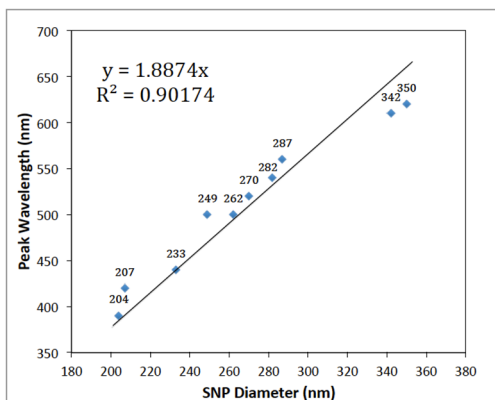


FIGURE 14.9

Scatter plot of the peak wavelength of the coloured samples in Figs. 14.8(A2)-8(E3) against the used SNP diameter with a best-fit linear function added

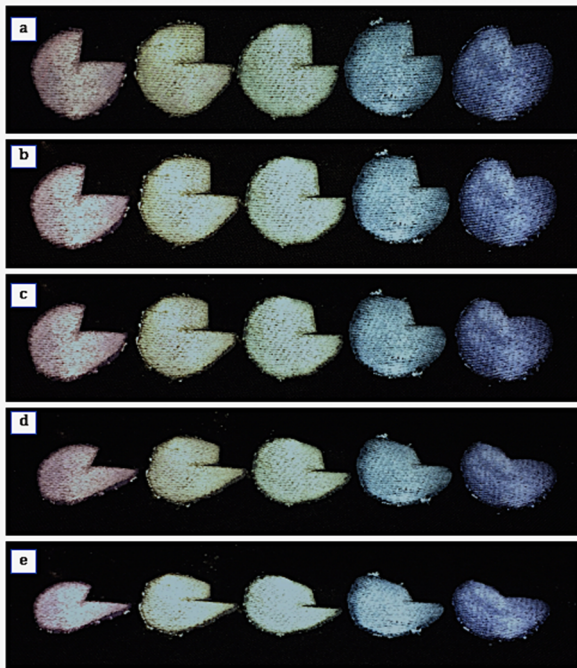


FIGURE 14.10

Images of SNP-coated BWC fabrics with viewing angles of 0° (a), 15° (b), 30° (c), 45° (d), and 60° (e). Samples in the vertical direction were treated with the same SNP batch solution. The fabric diameter is 25 mm, the right top of each circular fabric was cut to provide samples for SEM examination

The long range ordered SNP structure formed on the flat glass substrate resulted in high-quality structure colour with iridescent (angle-dependent) effects, Fig. 14.6. This is seen in natural precious opals, due to Bragg's Law Eq. (3), the varying of the viewing angle must lead to a change of the reflected wavelength due to Bragg diffraction. Many groups have produced high-quality photonic crystals on textile fabrics, and the iridescent colour effect [16][39][40] is usually observed. However, the colour changing property is less desirable for textile coloration, a stable colour is the essential requirement for real dyes and pigments. In this work, non-iridescent (angle-independent) structural colours were produced on circular black woven cotton fabrics, Figs. 14.8(A3)-8(E3). The images of these fabric samples at different viewing angles from 0 to 60 degrees at 15 degree intervals are shown in Fig. 14.10 [37]. It can be seen from Fig. 14.10 that the hue of the fabric is constant regardless of the viewing angle for all batches. The non-iridescent colour effect is from the short-range order [41] of the SNP photonic crystals on the fabric, where the Bragg diffraction of ordered regions and Mie scattering of disordered regions exist simultaneously.

The structural colours produced on the fabric substrate are shown in Figs. 14.8(A2) to 8(E5). The hue property is determined by the SNP diameter with other factors that affect the quality of the colours produced listed below:

1) fabric size: during the self-assembly process, smaller fabric samples tilt upward during the drying of the solvent at high temperatures. Therefore different areas receive different amounts of particles, resulting in non-uniform structural colours as seen in Figs. 14.8(A2)-8(E2); for a larger piece of fabric, it was much easier to retain a flat surface, the SNPs can be evenly deposited on the fabric surface, thus a more uniform structural colour will be produced, as seen in Figs. 14.8(A3)-8(E3);

2) fabric structure: compared with the woven structure ($0.034\text{g}/\text{cm}^2$ in this case), the knitted structure ($0.016\text{g}/\text{cm}^2$ in this case) is looser and more flexible, the knitted loop expands when drying the SNP suspension at high temperatures, this causes more SNPs to pass through the gaps between the yarns. The coverage of the SNPs onto the fabric is reduced accordingly, therefore the structural colour on the knitted fabric was less uniform as shown in Figs. 14.8(A4)-8(E4);

3) fabric colour: the self-assembly of SNPs on the pieces of white fabric did not give any structural colours perceptible to the observer regardless of the particle diameter, refer to Fig. 14.8(A5)-8(E5). The SEM images (Fig. 14.11) show that the SNPs did cover the surface of the knitted fabric (Fig. 14.11(a)), and both ordered SNP blocks and disordered regions were identified (Fig. 14.11(b) and 11(c)), just as seen from the SNP-coated knitted woven fabric, Fig. 14.7(b). This was probably due to the high reflection of the white background colour of the fabric, interfering with the structural colour from the Bragg diffraction.

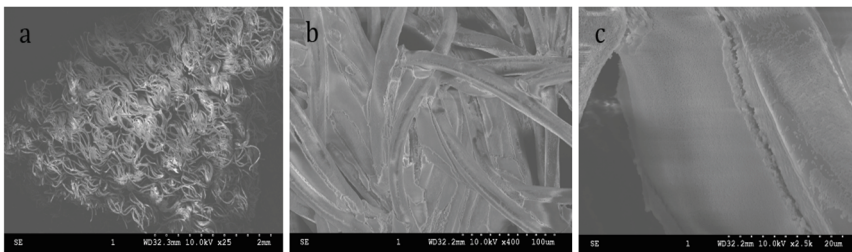


FIGURE 14.11

SEM images of white knitted nylon fabric shown in Fig. 14.8(C5), treated with 262 nm-sized SNPs, at different magnifications of 25 (a), 400 (b), and 2.5K (c)

Conclusion and outlook

Natural precious opals consisting of uniform tiny silica spheres provide a template for making artificial opal materials with tunable structural colours. In this work, uniform spherical silica nanoparticles have been produced using a novel solvent varying method based on the sol-gel Stöber process. The size and uniformity of the SNPs can be well controlled by only varying the initial volume of solvent ethanol. The self-assembly of silica spheres with diameters in the range of 200 nm to 350 nm on either glass or textile substrates resulted in structurally coloured opal films over the full visible spectrum. Generally, the structural colours on the flat glass substrates were more intense and uniform than those on the textured fabrics, which was due to the long-range ordering of SNPs on the glass. However, the SNPs that self-assembled on the fabrics have a short-range order because of the unevenness of the fabric surface. The non-iridescent structural colour effect on the fabric was due to the combination of Bragg diffraction of the ordered SNP blocks and the Mie scattering of disordered SNPs. It was determined that the quality of the structural colour on the fabric is affected by the fabric size, fabric structure, and fabric background colour. It can be concluded that a larger sized fabric with a tight woven structure and a dark background colour could obtain a relatively high-quality and uniform structural colour. This strategy of colouring textile materials using environmental friendly silica is promising for textile coloration without using any traditional dyes and/or pigments. Additional functionalities on textile materials such as hydrophobicity, UV protection, or auto-cooling could be achieved by the coating of such nanostructures through self-assembly techniques.

Acknowledgement

We would like to gratefully acknowledge the Startup Foundation of Shanghai University of Engineering Science (Grant Number: E3-0501-17-01093) and the Main Bursary of the Society of Dyers and Colourists (Grant Number: July 2014) to fund part of the research.

References

1. Kinoshita S (2008) Structural colors in the realm of nature. World Scientific.
2. Marlow F, Sharifi P, Brinkmann R, Mendive C (2009) Opals: status and prospects. *Angew Chem Int Ed Engl* 48:6212–6233. doi: 10.1002/anie.200900210.
3. Darragh PJ, Gaskin AJ, Sanders J V. (1976) Opals. *Sci Am* 234:84–95. doi: 10.1038/scientificamerican.0476-84.
4. Sanders JV (1964) Colour of precious opal. *Nature* 204:1151–1153. doi: 10.1038/2041151a0.
5. Jiang P, Bertone J (1999) Single-crystal colloidal multilayers of controlled thickness. *Chem Mater* 11:2132–2140. doi: 10.1021/cm990080+.
6. Mayoral R, Requena J, Moya JS, et al (1997) 3D Long-range ordering in an SiO₂ submicrometer-sphere sintered superstructure. *Adv Mater* 9:257–260. doi: 10.1002/adma.19970090318.
7. Park SH, Qin D, Xia Y (1998) Crystallization of mesoscale particles over large areas. *Adv Mater* 10:1028–1032. doi: 10.1002/(SICI)1521-4095(199809)10:13<1028::AID-ADMA1028>3.0.CO;2-P.
8. Jiang P, McFarland MJ (2004) Large-scale fabrication of wafer-size colloidal crystals, macroporous polymers and nanocomposites by spin-coating. *J Am Chem Soc* 126:13778–86. doi: 10.1021/ja0470923.
9. Park J, Moon J (2006) Control of colloidal particle deposit patterns within picoliter droplets ejected by ink-jet printing. *Langmuir* 22:3506–13. doi: 10.1021/la053450j.
10. Cheng B, Ni P, Jin C, et al (1999) More direct evidence of the fcc arrangement for artificial opal. *Opt Commun* 170:41–46. doi: 10.1016/S0030-4018(99)00434-4.
11. Gao W (2016) The Fabrication of Structurally Coloured Textile Materials Using Uniform Spherical Silica Nanoparticles. doi: 10.13140/RG.2.2.25724.54403.
12. Braun P V (2011) Materials science: Colour without colourants. *Nature* 472:423–4. doi: 10.1038/472423a.
13. Finlayson CE, Goddard C, Papachristodoulou E, et al (2011) Ordering in stretch-tunable polymeric opal fibers. *Opt Express* 19:3144. doi: 10.1364/OE.19.003144.
14. Yuan W, Zhou N, Shi L, Zhang K-Q (2015) Structural Coloration of Colloidal Fiber by Photonic Band Gap and Resonant Mie Scattering. *ACS Appl Mater Interfaces* 7:14064–71. doi: 10.1021/acsami.5b03289.
15. Shang S, Liu Z, Zhang Q, et al (2015) Facile fabrication of a magnetically induced structurally colored fiber and its strain-responsive properties. *J Mater Chem A* 3:11093–11097. doi: 10.1039/C5TA00775E.
16. Diao YY, Liu XY (2012) Bring Structural Color to Silk Fabrics. *Adv Mater Res* 441:183–186. doi: 10.4028/www.scientific.net/AMR.441.183.

17. Diao YY, Liu XY, Toh GW, et al (2013) Multiple structural coloring of silk-fibroin photonic crystals and humidity-responsive color sensing. *Adv Funct Mater* 23:5373–5380. doi: 10.1002/adfm.201203672.
18. Zhou L, Wu Y, Liu G, et al (2015) Fabrication of high-quality silica photonic crystals on polyester fabrics by gravitational sedimentation self-assembly. *Color Technol* 131:413–423. doi: 10.1111/cote.12164.
19. Zhou L, Liu G, Wu Y, et al (2014) The synthesis of core-shell monodisperse P(St-MAA) microspheres and fabrication of photonic crystals Structure with Tunable Colors on polyester fabrics. *Fibers Polym* 15:1112–1122. doi: 10.1007/s12221-014-1112-0.
20. Liu Z, Zhang Q, Wang H, Li Y (2011) Structural colored fiber fabricated by a facile colloid self-assembly method in micro-space. *Chem Commun* 47:12801–12803. doi: 10.1039/c1cc15588a.
21. Zhou N, Zhang A, Shi L, Zhang K-Q (2013) Fabrication of Structurally-Colored Fibers with Axial Core–Shell Structure via Electrophoretic Deposition and Their Optical Properties. *ACS Macro Lett* 2:116–120. doi: 10.1021/mz300517n.
22. Sun X, Zhang J, Lu X, et al (2015) Mechanochromic photonic-crystal fibers based on continuous sheets of aligned carbon nanotubes. *Angew Chem Int Ed Engl* 54:3630–4. doi: 10.1002/anie.201412475.
23. Tilley RJD (2010) Colour and the optical properties of materials. doi: 10.1002/9780470974773.
24. Gao W, Rigout M, Owens H (2016) Self-assembly of silica colloidal crystal thin films with tuneable structural colours over a wide visible spectrum. *Appl Surf Sci* 380:12–15. doi: 10.1016/j.apsusc.2016.02.106.
25. Stöber W, Fink A, Bohn E (1968) Controlled growth of monodisperse silica spheres in the micron size range. *J Colloid Interface Sci* 26:62–69. doi: 10.1016/0021-9797(68)90272-5.
26. Bogush GH, Tracy MA, Zukoski CF (1988) Preparation of monodisperse silica particles: Control of size and mass fraction. *J Non Cryst Solids* 104:95–106. doi: 10.1016/0022-3093(88)90187-1.
27. Nozawa K, Gailhanou H, Raison L, et al (2005) Smart control of monodisperse Stöber silica particles: effect of reactant addition rate on growth process. *Langmuir* 21:1516–1523. doi: 10.1021/la048569r.
28. Xia Y, Gates B, Yin Y, Lu Y (2000) Monodispersed colloidal spheres: old materials with new applications. *Adv Mater* 12:693–713. doi: 10.1002/(SICI)1521-4095(200005)12:10<693::AID-ADMA693>3.3.CO;2-A.
29. Gao W, Rigout M, Owens H (2016) Facile control of silica nanoparticles using a novel solvent varying method for the fabrication of artificial opal photonic crystals. *J Nanoparticle Res*. doi: 10.1007/s11051-016-3691-8.
30. Nassau K (2001) *The physics and chemistry of color: the fifteen causes of color*, 2nd Editio. Wiley.
31. Fudouzi H (2004) Fabricating high-quality opal films with uniform structure over a large area. *J Colloid Interface Sci* 275:277–283. doi: 10.1016/j.jcis.2004.01.054.
32. Sinitskii AS, Knotko A V., Tret'yakov YD (2005) Synthesis of SiO₂ Photonic Crystals via Self-organization of Colloidal Particles. *Inorg Mater* 41:1178–1184. doi: 10.1007/s10789-005-0283-x.
33. Ethanol-viscosity table and viscosity chart. <http://www.viscopedia.com/viscosity-tables/substances/ethanol/>.

34. Fu Y, Jin Z, Liu Z, et al (2008) Self-assembly of colloidal crystals from polystyrene emulsion at elevated temperature by dip-drawing method. *Mater Lett* 62:4286–4289. doi: 10.1016/j.matlet.2008.07.004.
35. Im SH, Park OO (2002) Effect of evaporation temperature on the quality of colloidal crystals at the water–air interface. *Langmuir* 18:9642–9646. doi: 10.1021/la025888e.
36. Liu G, Shao J, Zhang Y, et al (2015) Self-assembly behavior of polystyrene/methacrylic acid (P(St-MAA)) colloidal microspheres on polyester fabrics by gravitational sedimentation. *J Text Inst* 106:1293–1305. doi: 10.1080/00405000.2014.998011.
37. Gao W, Rigout M, Owens H (2017) Optical properties of cotton and nylon fabrics coated with silica photonic crystals. *Opt Mater Express* 7:341–353. doi: 10.1364/OME.7.000341.
38. Gao W, Rigout M, Owens H (2017) The structural coloration of textile materials using self-assembled silica nanoparticles. *J Nanoparticle Res* 19:303. doi: 10.1007/s11051-017-3991-7.
39. Shao J, Zhang Y, Fu G, et al (2014) Preparation of monodispersed polystyrene microspheres and self-assembly of photonic crystals for structural colors on polyester fabrics. *J Text Inst* 105:938–943. doi: 10.1080/00405000.2013.865864.
40. Liu G, Zhou L, Wu Y, et al (2015) Optical properties of three-dimensional P(St-MAA) photonic crystals on polyester fabrics. *Opt Mater (Amst)* 42:72–79. doi: 10.1016/j.optmat.2014.12.022.
41. Shi L, Zhang Y, Dong B, et al (2013) Amorphous photonic crystals with only short-range order. *Adv Mater* 25:5314–5320. doi: 10.1002/adma.201301909.